



BEHAVIOR OF PRECAST HIGH-PERFORMANCE FIBER REINFORCED CEMENT COMPOSITE COUPLING BEAMS UNDER LARGE DISPLACEMENT REVERSALS

B. Afsin CANBOLAT¹, Gustavo J. PARRA-MONTESINOS², and James K. WIGHT³

SUMMARY

In a coupled-wall structure, the behavior of coupling beams significantly affects the overall system efficiency and performance. Well designed coupling beams can substantially enhance the strength, stiffness, and energy dissipation of the coupled walls compared to individual walls. In order to ensure this desired behavior, current design provisions for the seismic design of reinforced concrete (RC) coupling beams in building codes require substantial reinforcement detailing, leading to reinforcement congestion and construction difficulties. In this study, an alternative approach for the design of coupling beams was investigated through the use of high performance fiber reinforced cementitious composites (HPFRCCs). These fiber cementitious materials exhibit a tensile strain hardening response after first cracking and a compression behavior that resembles that of well confined concrete. Three HPFRCC coupling beams reinforced with either polyethylene (PE) or twisted steel (Torex) fibers were tested under displacement reversals and their behavior was compared with that of a diagonally reinforced RC coupling beam. A precast construction process was proposed to provide time and workmanship savings, as well as good material quality control. Test results showed that HPFRCC coupling beams exhibit significantly higher shear strength, exceeding the upper limit allowed in the ACI Code, compared to RC coupling beams. The tension strain-hardening behavior and multiple cracking pattern exhibited by HPFRCC materials reduce the reliance on heavily reinforced diagonal cages for shear resistance; however, diagonal reinforcement is still necessary in order to achieve adequate displacement capacity. Moreover, superior damage tolerance of HPFRCC materials under large deformations provide adequate confinement to the diagonal bars at high drift levels, leading to the total elimination of the transverse reinforcement required around the diagonal reinforcement cages in RC coupling beams.

¹Ph.D. Candidate, ²Asst. Professor, ³Professor, Department of Civil and Environmental Engineering, University of Michigan, Ann Arbor, USA.

INTRODUCTION

Structural walls are widely used to provide earthquake resistance in medium-rise reinforced concrete (RC) buildings. In many design situations, structural walls feature rows of openings to add space usage flexibility, resulting in several walls generally connected by deep coupling beams. A coupled wall system is more efficient and economical than individual walls because properly designed coupling beams significantly increase the strength, stiffness, and energy dissipation capacity of the system. In an individual structural wall, most of the inelastic activity occurs within a limited plastic hinge region at the base of the wall. In a coupled wall system, coupling beams undergo significant inelastic deformation, spreading energy dissipation throughout the height of the structure. Therefore, the efficiency of a coupled wall system is dependent on the behavior of coupling beams under large flexural and shear deformations [1-4].

Test results have shown that large displacement and energy dissipation capacity cannot be attained in deep coupling beams with conventional detailing consisting of distributed horizontal and vertical reinforcement [1]. Therefore, an improved reinforcement scheme was developed for deep coupling beams [5] consisting of a group of diagonal reinforcing bars confined by closely spaced transverse reinforcement. Results from experimental research have shown that diagonally reinforced coupling beams are able to maintain their shear strength with good stiffness retention and energy dissipation capacity under large load reversals [5, 6]. However, diagonal reinforcement detailing creates construction difficulties due to reinforcement congestion problems associated with the placement of diagonal bars and closely spaced transverse reinforcement. Alternative reinforcement schemes have been investigated [7-9], such as rhombic reinforcement layout, the addition of dowels, or diagonal reinforcement only at the beam-wall interface. However, it was experimentally shown that coupling beams with those reinforcement alternatives exhibited inadequate seismic behavior and/or posed construction difficulties. Another alternative, consisting of steel or concrete encased steel coupling beams, has also been investigated [10]. Test results indicated that steel and hybrid coupling beams perform adequately under reversed cyclic loading. However, hybrid and steel coupling beam to RC wall connections have the potential to exhibit a bearing failure, resulting in less effective seismic performance.

With the recent developments in the field of fiber reinforced cement composites (FRCCs) [11-14], strain hardening or high-performance fiber reinforced cement composites (HPFRCCs) are now a viable alternative to regular concrete in shear critical members. These materials exhibit multiple cracking under uniaxial tension and a compression behavior that resembles that of well confined concrete. Beyond the tensile strain at post-cracking strength, damage localization occurs due to fiber pullout. The use of HPFRCCs has been experimentally investigated in seismic-resistant structural members, such as low-rise walls [15], RCS beam-column joints [16], connections for precast concrete frames [17, 18], and plastic hinge regions in bridge piers [19]. In those applications, it was shown that HPFRCC members are able to withstand significantly higher deformations with superior damage tolerance and bond properties compared to RC members.

In this research project, the seismic behavior of HPFRCC coupling beams was investigated. With the use of HPFRCC materials, the reliance on heavily reinforced diagonal cages and the need for confinement reinforcement were expected to be reduced or eliminated. The experimental phase of this research consisted of the testing of three large-scale HPFRCC coupling beams and one diagonally reinforced RC coupling beam under displacement reversals. The main variables investigated were the type of material used in the coupling beams, fiber type, and reinforcement detailing. A precast construction process was proposed because site casting of HPFRCC coupling beams may be difficult for a typical concrete contractor. The precast HPFRCC beams are constructed with sufficient embedment length and reinforcement anchorage to assure proper moment and shear transfer. Then, they are placed between the

walls and regular concrete is cast around them (Fig. 1). This construction process is expected to be practical and attractive for industry because it will not only lead to significant savings in time and workmanship at the site, but also provide good material quality control.

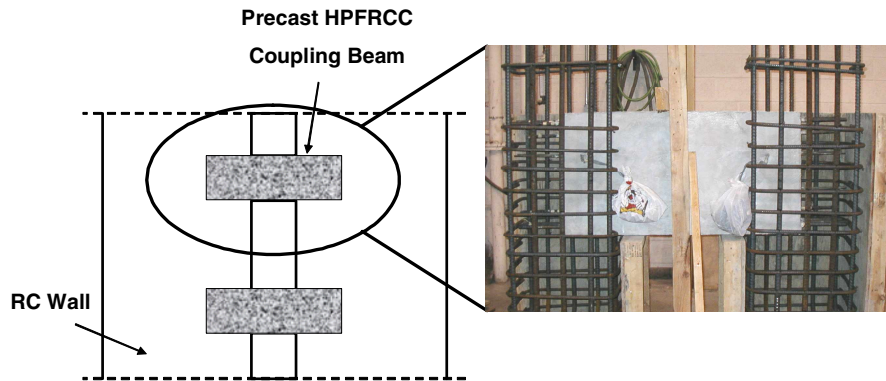


Figure 1 – Proposed Precast HPFRCC Coupling Beams

EXPERIMENTAL PROGRAM

Test Specimens and Setup

In this experimental program, the feasibility of using HPFRCC materials to simplify reinforcement detailing in seismic-resistant RC coupling beams was evaluated. For this purpose, four coupling beam specimens, including a control RC specimen, were tested under large displacement reversals. As shown in Fig. 2, each specimen consisted of a coupling beam and two stiff RC members representing structural walls. The beam dimensions were proportioned to approximately 3/4 of full scale. After being constructed, the specimens were rotated and one of the walls was connected to a strong floor. In this horizontal position, displacement cycles were applied at the other (top) wall portion through a horizontal hydraulic actuator with its line of action passing through the beam midspan in order to produce an antisymmetrical moment pattern in the coupling beam. The actuator and the upper portion of the specimen were connected through a steel I-section and the load was transferred to the top RC block (RC wall) by means of direct bearing and unbonded threaded bars passing through the top block. The test specimens were braced laterally to prevent out-of-plane movements.

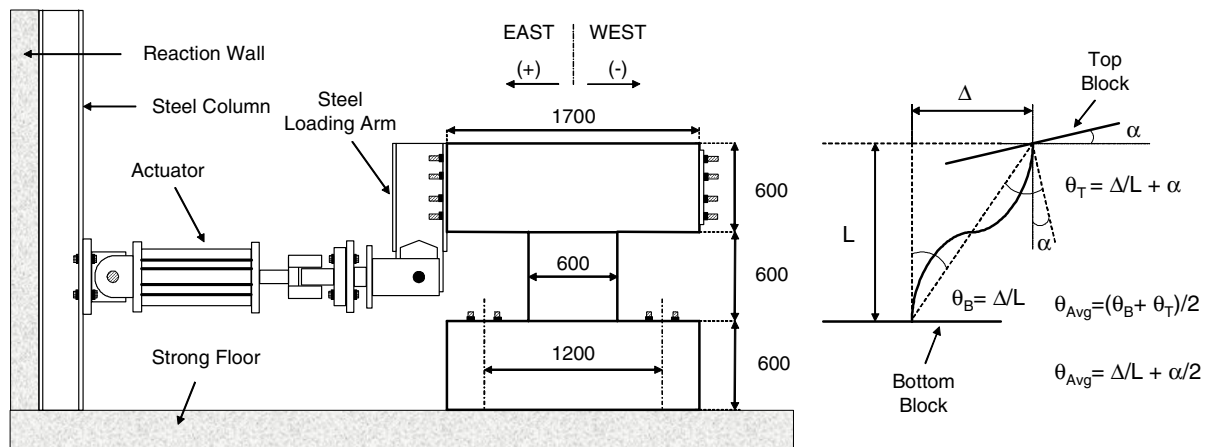


Figure 2 – Specimen Dimensions (mm) and Test Setup

The specimens were subjected to quasi-static cyclic loading in a displacement control mode, following a predefined reversed cyclic displacement pattern. To simulate the demands during an earthquake, several lateral displacement cycles were applied to each specimen, starting from a coupling beam drift of 0.25%, and reaching a maximum drift of 4% (provided that the specimen did not fail at a lower drift level). Each cycle to a given drift level was applied twice to evaluate the loss of strength and stiffness in the specimens during the repeated cycles. Some 0.5% drift cycles were interspersed into the displacement history to evaluate the residual stiffness of the specimens. The horizontal displacement reached at each drift level was monitored through linear potentiometers because LVDT readings from the hydraulic actuator were inaccurate due to deformations in the loading system. Additional potentiometers were also used to check any relative rotation between the RC walls. The lateral displacement applied to the specimens was then based on the calculation of a net beam drift (θ_{Avg}) obtained through the potentiometer readings and taking into account the effect of wall rotation on coupling beam drift (Fig. 2).

The primary experimental parameters evaluated in this project were the type of cement-based material used in the coupling beams, fiber type, and reinforcement detailing. The design parameters and corresponding values are given in Table 1. A span-to-depth ratio of 1.0 was selected for the coupling beams in order to ensure a shear dominant behavior. As the span-to-depth ratio increases, flexural deformations will play a more significant role, and thus the drift capacities obtained in this investigation could be considered a lower bound for most practical coupling beam aspect ratios.

Table 1 - Description of Test Specimens

Specimen	Diagonal Reinforcement	Cement-based Material	Span-to-Depth Ratio	Horizontal /Vertical Reinforcement Ratio
1	Yes	Concrete	1.0	0.25% / 0.25%
2	No	HPFRCC (PE)	1.0	0.25% / 0.25%
3	Yes*	HPFRCC (PE)	1.0	0.25% / 0.25%
4	Yes*	HPFRCC (Torex)	1.0	0.25% / 0.60%

* No transverse reinforcement used to confine diagonal bars

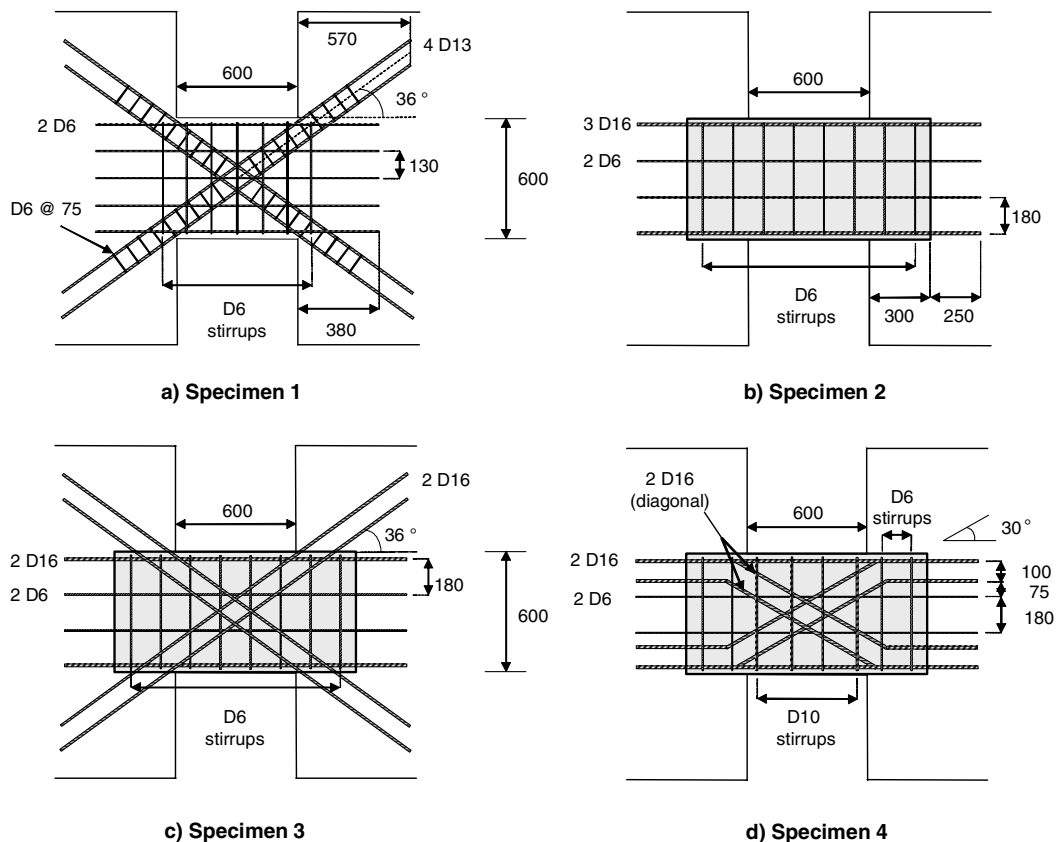
Specimen 1, used as the control specimen, consisted of a 200 mm (8 in.) wide RC coupling beam with diagonal reinforcement designed and detailed according to the ACI 318 Code [20]. Minimum code requirements for distributed horizontal and vertical reinforcement were applied to increase the demand in the diagonal bars. Fig. 3a shows a sketch of the details used in Specimen 1.

In Specimen 2, a precast HPFRCC coupling beam was constructed with no diagonal reinforcement. The shear capacity was provided by a HPFRCC material containing a 2.0% volume fraction of ultra-high molecular weight polyethylene (PE) fibers and minimum distributed horizontal and vertical reinforcement. Sufficient flexural reinforcement was provided at the top and bottom layers in order to enforce a diagonal tension failure. Also, because of the elimination of diagonal bars and corresponding hoops, the beam width in Specimen 2 was reduced to 150 mm (6 in.) in order to increase the shear demand in the composite material. The reinforcement details of Specimen 2 are shown in Fig. 3b. The precast coupling beam was embedded a distance equal to half its span length into each wall to reduce bearing stresses, and the horizontal reinforcing bars were extended beyond the ends of the beam to provide full development length from the face of the wall (Fig. 3b).

Specimen 3 consisted of a precast HPFRCC coupling beam with the same beam width and amount of distributed horizontal and vertical reinforcement as in Specimen 2. However, two D16 diagonal bars with no confining reinforcement, which corresponded to approximately 80% of the area of diagonal reinforcement used in Specimen 1, were placed in each direction (Fig. 3c). With this configuration, it was

intended to evaluate the interaction between HPFRCC and diagonal bars, as well as the contribution of the diagonal bars to the strength, displacement, and energy dissipation capacity of HPFRCC coupling beams.

Specimen 4 contained the same amount of diagonal bars used in Specimen 3. However, the diagonal reinforcement detailing was modified to facilitate the construction process for a precast coupling beam. As shown in Fig. 3d, the bars ran diagonally within the beam span and were bent at the beam-wall interface so that they would remain within the depth of the beam. A new composite material, consisting of a cement-based mortar with twisted steel (Torex) fibers [14] in a 1.5% volume fraction, and minimum distributed horizontal reinforcement were used in the coupling beam, but the distributed vertical reinforcement within the beam span was increased to prevent a premature failure at the bending points of the diagonal bars. The beam width was kept the same as in the other HPFRCC coupling beam specimens (150 mm).



Dimensions in mm. Concrete cover = 50 and 40 mm for RC and HPFRCC specimens, respectively.

Figure 3 - Reinforcement Details of Test Specimens

Material Properties

Recent experimental studies have indicated that HPFRCCs can exhibit a ductile response in tension similar to strain hardening behavior of metals [13]. In plain concrete, first cracking results in a rapid loss of tensile strength. In fiber cementitious composites with strain hardening response, however, fibers bridging initial tension cracks carry an increasing amount of force across these cracks, leading to the formation of multiple cracks in the composite. This crack formation process continues until the peak bridging stress is reached on one of the cracks, leading to a wide opening of that crack. At higher deformations, damage is localized on this particular crack and the composite tensile strength diminishes gradually. In the end, a highly ductile tensile performance is achieved with a multiple cracking pattern and

significant damage tolerance. Achieving this tensile performance is primarily related to the volume fraction of the fibers in the composite, fiber material and geometry, cementitious matrix composition, average bond strength at the fiber-matrix interface, and homogeneous distribution of fibers in the matrix.

In this research study, different mix designs were considered for use in the coupling beams and several specimens were tested in order to evaluate the tensile and compression response of the composite. Dogbone-shaped specimens of two different sizes were used for uniaxial tension tests. Two fiber cementitious materials with the desired multiple cracking behavior in tension were obtained using a 2.0% volume fraction of PE fibers, and a 1.5% volume fraction of Torex fibers. PE fibers are made of ultra-high molecular weight polyethylene, widely used in fiber reinforced plastics for the aerospace industry. A typical tensile stress vs. strain response obtained from a dogbone specimen with PE fibers is shown in Fig. 4. Torex is a twisted steel fiber with excellent frictional and mechanical bond properties [14]. Table 2 lists the properties of the PE and Torex fibers used in this research.

Table 2 – Fiber Properties

Fiber Type	Material	Tensile Strength MPa (ksi)	Elastic Modulus GPa (ksi)	Diameter mm (in.)	Length mm (in.)	Volume in composite (%)
PE	UHMWPE*	2570 (375)	117 (17000)	0.038 (0.0015)	13 (0.5)	2.0
Torex	Steel	2470 (360)	200 (29000)	0.3 (0.012)	30 (1.2)	1.5

- Ultra-High Molecular Weight Polyethylene

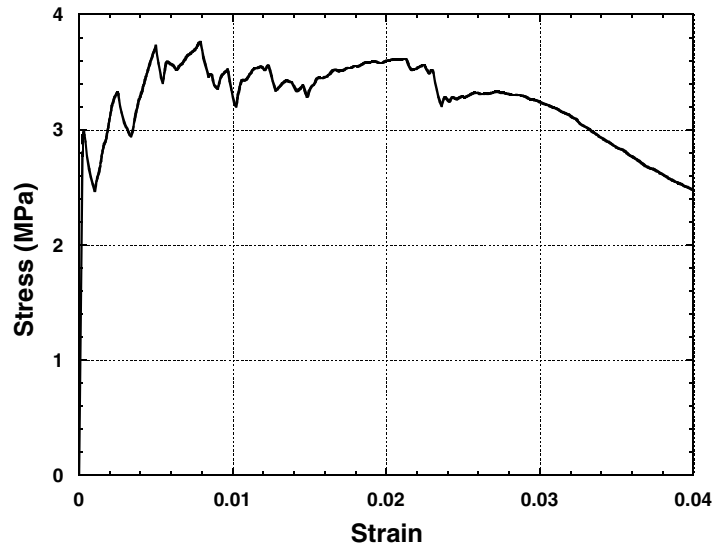


Figure 4 - Typical Tensile Stress vs. Strain Response of Sample Specimen with PE Fibers

The compressive strengths for the composites with PE and Torex fibers at test day were approximately 57 MPa (8300 psi) and 63 MPa (9100 psi), and the post-cracking tensile strengths were approximately 3.1 MPa (450 psi) and 5.5 MPa (800 psi), respectively. Regular concrete, provided by a local ready-mix concrete supplier, was used in the coupling beam of the first specimen and in the walls of all four specimens. The concrete compressive strength for Specimen 1 on the test day was approximately 41 MPa (6000 psi). All the deformed steel reinforcement used in this study was Grade 60 (420 MPa). Tensile test results indicated a yield stress of 450 MPa (65 ksi) and a tensile strength of 726 MPa (105 ksi).

EXPERIMENTAL RESULTS

Shear Force-Drift Response

Table 3 summarizes the experimental results in terms of maximum load and corresponding beam shear stress, both numerical and as a multiple of $\sqrt{f'_c}$ to compare with ACI code limit of $\frac{5}{6}\sqrt{f'_c}$ (MPa) [20].

Table 3 - Strength of Test Specimens

Specimen	Max. Force kN (kips)	Shear Stress MPa (psi)	Shear Stress ($\sqrt{f'_c}$) MPa (psi)
1	470 (105)	3.8 (550)	0.6 (7.1)
2	600 (135)	6.2 (900)	0.8 (10)
3	800 (180)	8.6 (1250)	1.15 (14)
4	800 (180)	8.6 (1250)	1.1 (13)

Also, Fig. 5 shows the shear force versus drift response of all four specimens. As mentioned before, the drift levels were adjusted to account for the differential rotation of the wall blocks. As can be seen from Fig. 5a, Specimen 1 had a stable response, which indicated that diagonally reinforced RC coupling beams designed according to the ACI Building Code perform well under high deformation demands. Yielding of the diagonal bars led to wide hysteresis loops with good energy dissipation capacity. In Specimen 1, the shear strength provided by the diagonal bars at yielding was approximately 270 kN, around 60% of the maximum load reached during the test. Therefore, it is likely that this contribution increased significantly during the later drift cycles due to strain hardening of the steel reinforcement.

Specimen 2 consisted of HPRCC coupling beam with PE fibers in a 2.0% volume fraction and no diagonal reinforcement was used. Fig. 5b shows that Specimen 2 exhibited a stable response up to 2.0% drift. However, the beam strength then dropped significantly due to damage localization, followed by fiber pullout. The hysteresis loops showed some “pinching” with less energy dissipation capacity compared to Specimen 1. This pinching is due to the fact that the PE fibers are effective in restraining crack opening, but once unloaded they do not provide any resistance against crack closing. In addition to that, the contribution of minimum distributed horizontal and vertical reinforcement to the force transfer mechanism across cracks during the crack closing process was very limited.

Shear strength reached by Specimen 2 was approximately 60% larger than that in Specimen 1 (Table 3). The shear strength provided by the HPRCC material was estimated based on the diagonal tension strength provided by the fibers bridging a diagonal crack spanning from one corner of the coupling beam to the other corner. From the post-cracking tensile strength of 3.1 MPa (450 psi) obtained for the HPRCC material used in Specimen 2, a shear strength contribution of 290 kN (65 kips) was estimated, which represents half of the strength observed in Specimen 2. This estimated fiber strength contribution is consistent with the strength loss that occurred when the major diagonal cracks formed after 2.0% drift. Up to the fiber pullout drift, Specimen 2 sustained a shear stress equal to the maximum limit permitted by ACI 318 Code [20] (Table 3).

The strength and displacement capacity of the coupling beam in Specimen 3 was significantly increased through the use of diagonal bars confined only by HPRCC material, as observed in Fig. 5c. In terms of strength, the diagonal bars were estimated to contribute approximately 210 kN (47 kips) of the beam shear strength at yielding (26% of maximum beam strength). Consistent with this expected strength, the difference in strength between Specimens 2 and 3 was about 200 kN (45 kips). The maximum load of 800

kN (180 kips) was recorded in Specimen 3 at about 2.5% drift. This peak load was maintained up to 4% drift in the positive direction, where a sudden drop of approximately 290 kN (65 kips) was observed due to the loss of diagonal tension strength in the HPCFRCC material. During subsequent loading cycles, the residual shear strength was below 450 kN (100 kips), and was primarily due to the shear carrying capacity provided by the diagonal bars and nominal beam transverse reinforcement. After the major diagonal cracks opened widely, the HPCFRCC material with PE fibers began losing its ability to support the diagonal bars. During the repeated cycle in the negative direction targeted to 4.0% drift, the diagonal bars under compression buckled, losing their load carrying capacity.

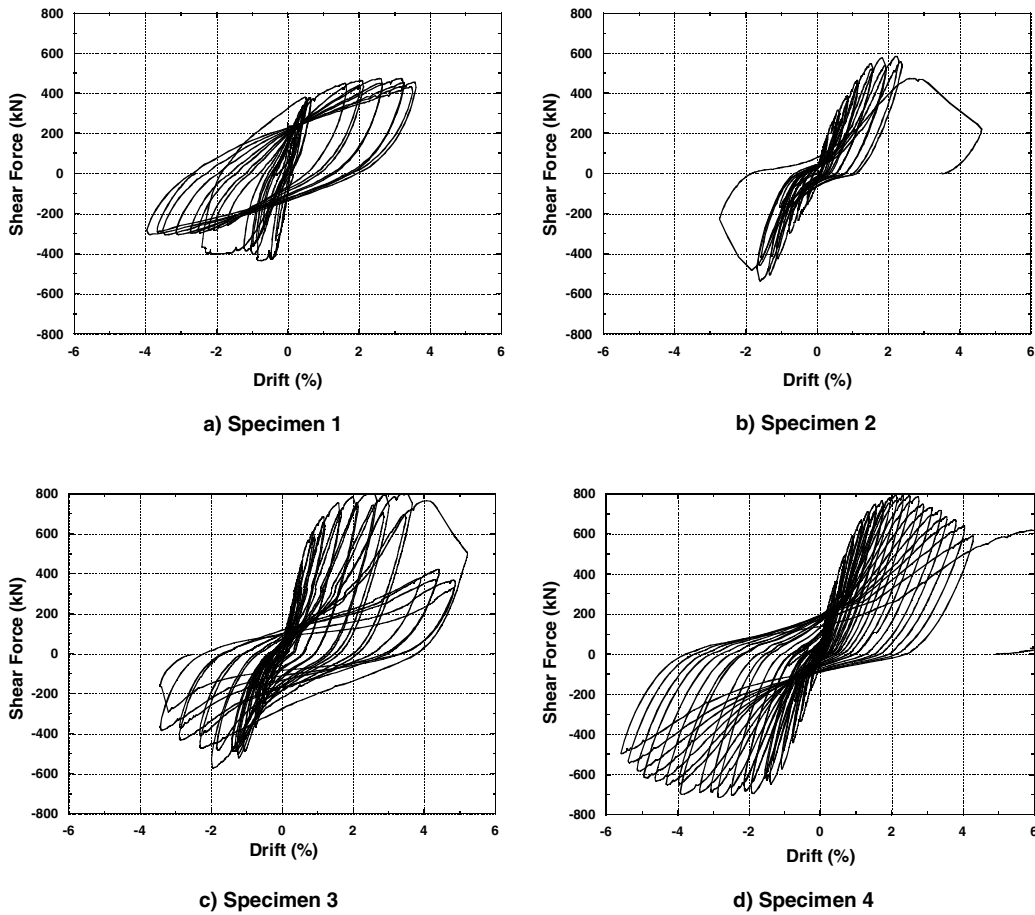


Figure 5 –Shear Force versus Drift Response of Test Specimens

The maximum average shear stress in Specimen 3 was around 230% of the peak shear stress measured in Specimen 1 and 40% larger than that of Specimen 2 (Table 3). With regard to displacement capacity, a maximum drift of approximately 4.0% was reached in Specimen 3, which is almost twice that of Specimen 2. It should be noted that extensive rotations in the top block affected the applied displacement history. As can be observed in Fig. 5c, the adjusted drift levels reached in the positive loading direction in Specimen 3 were larger than those in the negative loading direction. The shape of the hysteresis loops indicated that the energy dissipation capacity of Specimen 3 was significantly larger than that of Specimen 2.

In Specimen 4, the cyclic displacement pattern was modified and single cycles were incremented by 0.25% for drifts larger than 2.0%, representing a more gradual increase in drift values. With this

modification in the displacement history, a better evaluation of the drift level at fiber pullout was intended. In addition to that, when a target displacement was reached, the displacement was not held constant to mark cracks, but the specimen was unloaded to prevent a sudden energy release due to fiber pullout. The shear force versus drift response given in Fig. 5d demonstrated that Specimen 4 had a very stable response with good energy dissipation, comparable to Specimen 3. Further, it was observed that the bent diagonal bars performed as well as the straight bars used in Specimen 3.

A maximum load of approximately 800 kN (180 kips) was measured in Specimen 4 at a drift of 2.0% in the positive loading direction. After this drift level, the contribution of the fiber cementitious material to coupling beam strength started to deteriorate. However, the strains in the diagonal bars were large enough to cause these bars to go into strain hardening, increasing reinforcement contribution to shear strength and leading to a gradual decrease in beam shear strength up to 4.0% drift. Specimen 4 was displaced up to 5.5% drift in the negative loading direction with a corresponding applied shear of approximately 70% of the peak load in that direction. At the end of the test, the specimen was displaced monotonically in the positive loading direction up to nearly 8.0% drift, at which point the diagonal bars fractured. The load measured at this drift level was approximately 80% of the peak load for that loading direction, indicating that the cementitious material was effective in supporting the diagonal bars even after opening of wide diagonal cracks. The shear stress demand in Specimen 4 was about the same as that in Specimen 3, which was significantly larger than the maximum allowable shear stress in the ACI 318 Code [20] for a coupling beam.

Fig. 6 shows a comparison between the shear stress versus drift responses for Specimens 1 and 4. As can be observed, Specimen 4 sustained shear stresses twice as large and possessed substantially larger energy dissipation capacity compared to Specimen 1.

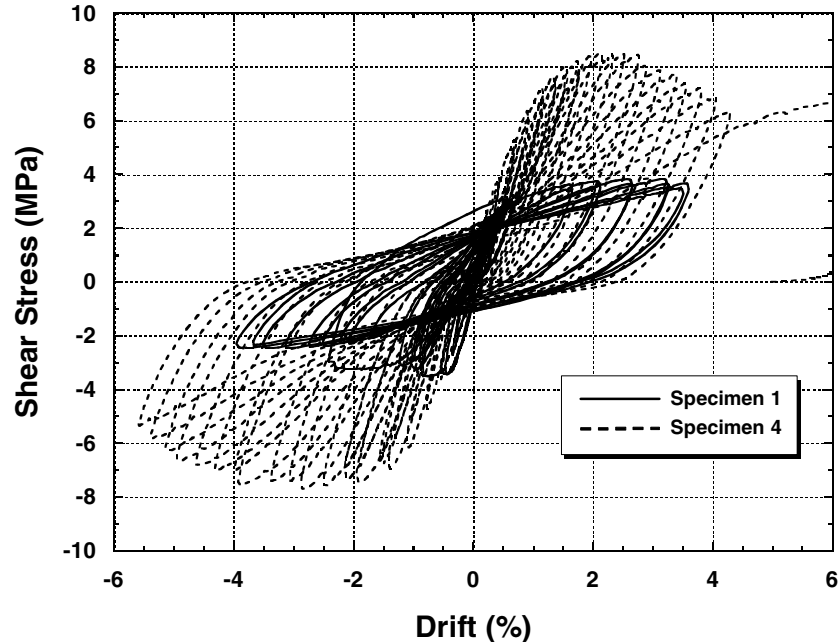


Figure 6 – Shear Stress versus Drift Response of Specimens 1 and 4

Cracking Pattern and Damage Progress

For Specimen 1, diagonal cracks began to form in the coupling beam during the cycles to 0.25% drift. These cracks widened substantially at 1.5% drift, reaching a state that could be classified as moderate damage (Fig. 7a). At drift levels larger than 2.5%, severe damage was observed in the coupling beam with concrete spalling and tensile strains in the diagonal reinforcement in excess of 1.5%. Fig. 7b shows the damage level in the RC coupling beam at 3.5% drift. Even though extensive cracking and damage had occurred at the maximum drift level of 4.0%, no clear indication of failure was observed.

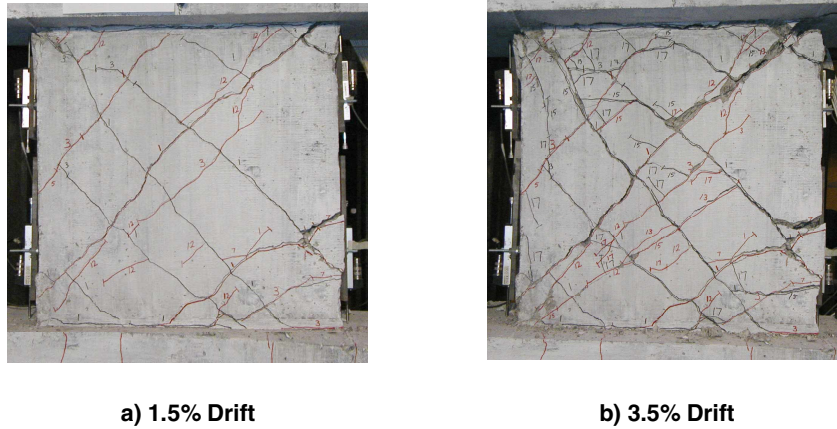


Figure 7 - Cracking Pattern in Specimen 1

In Specimen 2, the first diagonal cracks also formed during the cycles to 0.25% drift. As the test progressed, several diagonal cracks propagated throughout the beam, as opposed to only a few diagonal cracks in the RC coupling beam. At 1.5% drift, the HPCFRCC coupling beam was crossed by tens of hairline diagonal cracks (Fig. 8a). At about 2.0% drift in the negative direction, fiber pullout occurred, leading to the opening of a wide diagonal crack (Fig. 8b) with a subsequent drop in beam strength. When the displacement was reversed, another diagonal crack, perpendicular to the previously formed crack, opened at approximately 3.0% drift and resulted in a diagonal tension failure of the coupling beam.

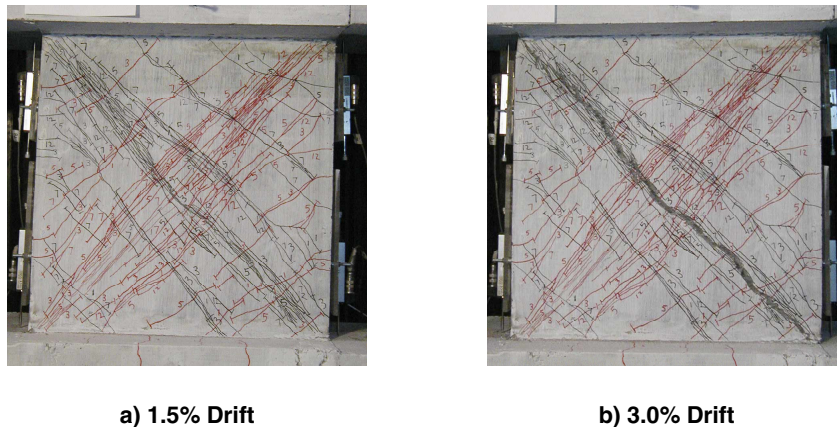


Figure 8 - Cracking Pattern in Specimen 2

Overall damage progress observed in Specimens 3 and 4 was similar to that of Specimen 2. Diagonal cracking began during the cycles to 0.25% drift and a large number of hairline cracks had formed when the 1.5% drift level was reached. At approximately 2.0% drift, damage localization initiated at a few diagonal cracks that spanned opposite corners in the coupling beam. However, contrary to the behavior of

Specimen 2, Specimens 3 and 4 carried the same or an increasing amount of load at drifts up to 4.0% due to the use of supplemental diagonal reinforcement. Figs. 9a and 9b show the cracking pattern in Specimens 3 and 4, respectively.



a) Specimen 3 at 4.0% Drift



b) Specimen 4 at 4.0% Drift

Figure 9 - Cracking Pattern in Specimens 3 and 4

Shear Distortion Response

The shear force versus shear distortion response for the four coupling beam specimens is shown in Fig. 11. Specimen 1, detailed as per the 1999 ACI 318 Code [20], exhibited a stable shear response throughout the test (Fig. 10a). Because the diagonal bars resisted most of the applied shear force, wide hysteresis loops were obtained. The maximum shear distortion measured in Specimen 1 was 1.5% (0.015 rad) at a drift of 4.0%, indicating that large flexural deformations dominated the coupling beam response.

As shown in Fig. 10b, a pinched shear distortion response was observed in Specimen 2 due to absence of an effective force transfer mechanism. During crack opening, PE fibers are only effective in transferring tensile forces between diagonal cracks. When the displacement (load) direction was reversed, the fibers did not resist the crack closing process, and thus only the nominal beam reinforcement contributed transferring forces across cracks. Once the diagonal cracks closed, the specimen regained its stiffness. The coupling beam in Specimen 2 had a shear distortion capacity of approximately 1.0%. At this distortion level, fiber pullout occurred, leading to a significant drop in the strength of the specimen.

In Specimens 3 and 4, the shear distortion capacity was significantly improved due to the presence of the diagonal bars. Specimen 3 sustained a shear distortion of approximately 2.5% in the positive loading direction before a significant drop in strength occurred (Fig. 10c). This large distortion, compared to Specimen 1, also indicates that shear deformations played a dominant role in the specimen response. In Specimen 4, the beam strength decay began before a 2.0% shear distortion as fiber pullout initiated (Fig. 10d). However, because of the increasing strength contribution from the diagonal bars as they strain hardened, the loss of beam shear strength was gradual. In this specimen, a maximum shear distortion of 3.0% was measured during the cycles to approximately 4.0-5.0% drift. During the final push, a shear distortion of 6.0% was measured, just before fracture of the diagonal reinforcement occurred.

In all three specimens constructed with a fiber cementitious material, only minor damage was observed at shear distortions of up to 1.0%. When diagonal reinforcement was provided to prevent a sudden failure after fiber pullout, a 1.5-2.0% shear distortion could be considered the limit for moderate damage. For larger shear distortions, damage localization with significant crack opening due to fiber pullout can be expected.

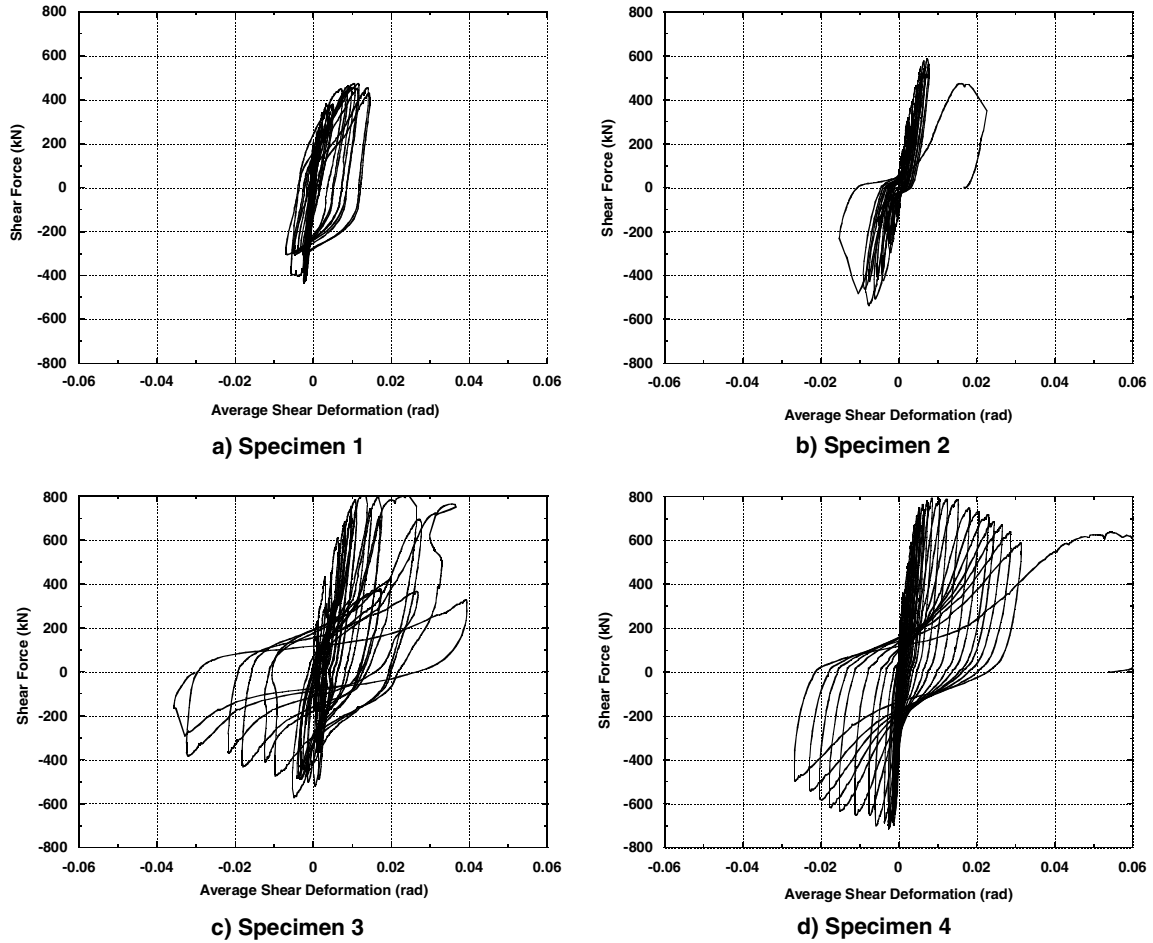


Figure 10 - Shear Force versus Distortion Response of Test Specimens

Energy Dissipation

The energy dissipation capacity of the HPFRCC coupling beams with diagonal reinforcement (Specimens 3 and 4) could be assumed to represent a lower bound because those coupling beams were designed to fail under diagonal tension with little flexural yielding. Therefore, in a typical design, larger energy dissipation capacity is expected by forcing large inelastic flexural deformations before opening of wide diagonal cracks.

As mentioned earlier, the shear force versus drift hysteresis loops give a visual indication of the energy dissipation capability of the specimens. From Fig. 5, it was observed that Specimen 1 had good energy dissipation with wide hysteresis loops, Specimen 2 experienced “pinching” due to lack of an efficient force transfer mechanism during unloading, and the supplemental diagonal bars used in Specimens 3 and 4 enabled better energy dissipation with respect to Specimen 2. Energy dissipated per cycle was determined for each specimen by calculating the area enclosed by the hysteresis loops in the shear force versus drift diagrams. To account for different drift levels reached for positive and negative loading directions in a cycle, average drift was used. Fig.11 shows the energy dissipated per cycle for Specimens 1 and 4 with respect to drift levels. As can be observed, the energy dissipation capacity of Specimen 4 was comparable to that of Specimen 1, even though the amount of diagonal reinforcement and beam width were less than that of Specimen 1. For both specimens, there is an almost linear increase in the energy dissipated from 1.5% to 4.0% drift. Beyond this point, energy dissipation per cycle remained constant for

Specimen 4 up to 5.0% drift. These findings indicate that HPFRCC coupling beams with simplified reinforcement detailing can exhibit a stable behavior with good energy dissipation.

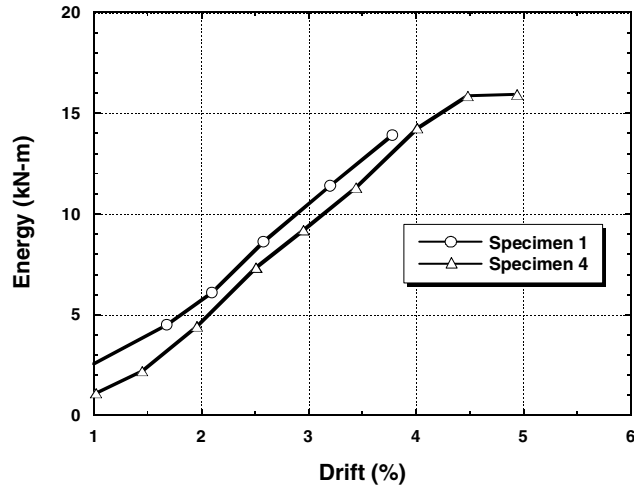


Figure 11 – Energy Dissipation per Cycle versus Drift Response for Specimens 1 and 4

Stiffness Retention

Fig. 12 shows the normalized stiffness versus drift response for all four specimens. The stiffness was a secant value measured from peak-to-peak displacement point in each direction. The stiffness values were normalized with respect to the secant stiffness at 0.25% drift in order to account for the variations in specimen parameters. From Fig.12, it can be observed that HPFRCC coupling beams showed better stiffness retention with respect to the RC coupling beam. Normalized stiffness of Specimen 1 decreased significantly after the formation of the first diagonal cracks, whereas the HPFRCC specimens showed a relatively gradual stiffness decrease up to at least 2.0% drift. At that drift level, fiber pullout occurred in Specimen 2, resulting in a sudden stiffness drop. The presence of diagonal reinforcement in Specimen 3 not only delayed this stiffness drop up to 4.0% drift, but also improved the stiffness retention at low drift values. When the normalized stiffness values at 2.0% drift for the four specimens are compared, it can be seen that Specimen 1 maintained only 20% of its initial stiffness, whereas the HPFRCC specimens maintained about 40% to 50% of their initial stiffness.

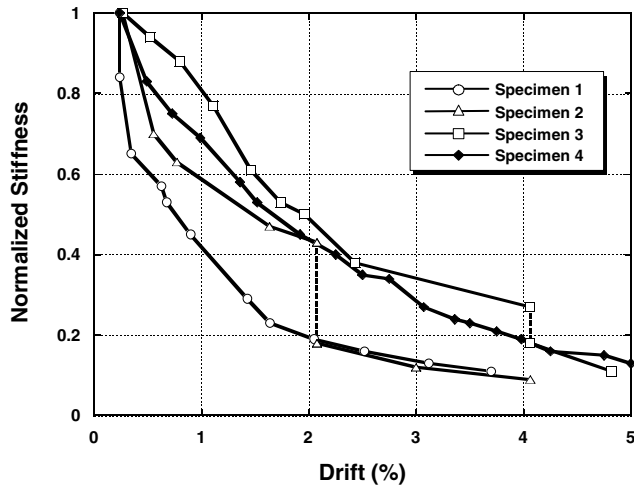


Fig. 12 – Normalized Stiffness versus Drift Response of Test Specimens

CONCLUSIONS

In this research program, the use of high performance fiber reinforced cementitious composites (HPFRCCs) in RC coupling beams was investigated to reduce diagonal reinforcement requirements, and thus the associated reinforcement congestion problems and construction difficulties. For this purpose, three HPFRCC coupling beams containing either ultra-high molecular weight polyethylene (PE) fibers or twisted steel (Torex) fibers were tested under reversed cyclic displacements and their behavior was compared with that of a diagonally reinforced RC coupling beam. A precast construction process was proposed for HPFRCC coupling beams to provide time and workmanship savings, as well as good material quality control.

The main variables investigated in this research were the type of cement-based material used in the coupling beams, i.e. regular concrete, HPFRCC with PE or twisted steel (Torex) fibers, and reinforcement detailing. The first specimen, used as the control specimen, consisted of an RC coupling beam with diagonal reinforcement designed and detailed according to the ACI 318 Code. In the second specimen, the coupling beam was constructed with a HPFRCC with PE fibers, and only conventional horizontal and vertical reinforcement was provided. Specimens 3 and 4 were constructed with HPFRCC containing PE and twisted steel (Torex) fibers, respectively, and supplementary diagonal bars with no confinement reinforcement were provided.

The performance of these new precast HPFRCC coupling beams under reversed cyclic loading demonstrated that a more convenient reinforcement detailing can be used in coupling beams and still maintain adequate seismic behavior. The use of advanced fiber cementitious materials allowed the elimination of the transverse reinforcement typically required around the diagonal bars for confinement, thus simplifying the beam construction process. Considering the multiple cracking pattern with only hairline diagonal cracks in the coupling beams up to 2% drift, it is clear that HPFRCC materials have superior damage tolerance under displacement reversals expected in a moderate earthquake. Test results at large drift levels showed that HPFRCC coupling beams with simplified diagonal reinforcement exhibited higher shear strength and stiffness retention. In addition, the HPFRCC beams with supplemental diagonal bars maintained about 80% of their shear strength up to at least 4.0%.

ACKNOWLEDGEMENT

This research study was sponsored by the National Science Foundation under Grant No. CMS 0001617. The conclusions contained in this paper are those of the authors and do not necessarily represent the views of the sponsor.

REFERENCES

1. Paulay, T. (1971), "Coupling Beams of Reinforced Concrete Shear Walls," Journal of the Structural Division, ASCE, Vol. 97, No. ST3, pp. 843-862.
2. Mahin, S.A., and Bertero, V.V. (1976), "Nonlinear Seismic Response of a Coupled Wall System," Journal of the Structural Division, ASCE, Vol. 102, No. 9, pp. 1759-1780.
3. Aktan, A.E., and Bertero, V.V. (1981), "The Seismic Resistant Design of R/C Coupled Structural Walls," Report No. UCB/EERC-81/07, Earthquake Engineering Research Center, University of California, Berkeley.
4. Munshi, J.A., and Ghosh, S.K. (2000), "Displacement-Based Seismic Design of Coupled Wall Systems," Earthquake Spectra, Vol. 16, No. 3, pp. 621-642.

5. Paulay, T., and Binney, J.R. (1974), "Diagonally Reinforced Coupling Beams," Special Publication SP-42, American Concrete Institute, Detroit, Michigan, pp. 579-598.
6. Paulay, T., and Santhakumar, A.R. (1976), "Ductile Behavior of Coupled Shear Walls," Journal of the Structural Division, ASCE, Vol. 102, No. ST1, pp. 93-108.
7. Tassios, T.P., Moretti, M., and Bezas A. (1996), "On the Behavior and Ductility of Reinforced Concrete Coupling Beams of Shear Walls," ACI Structural Journal, Vol. 93, No.6, pp. 711-720.
8. Galano, L., and Vignoli, A. (2000), "Seismic Behavior of Short Coupling Beams with Different Reinforcement Layouts," ACI Structural Journal, Vol. 97, No. 6, pp. 876-885.
9. Tegos, I.A., and Penelis, G.Gr. (1988), "Seismic Resistance of Short Columns and Coupling Beams Reinforced with Inclined Bars," ACI Structural Journal, Vol. 85, No. 1, pp. 82-88.
10. Gong, B., Shahrooz, B.M., and Gillum, A.J. (1998), "Cyclic Response of Composite Coupling Beams," Special Publication SP-174, American Concrete Institute, Farmington Hills, Michigan, pp. 89-112.
11. Naaman, A.E., and Reinhardt, H.W. (1996), "Characterization of High Performance Fiber Reinforced Cement Composites – HPFRCC," High Performance Fiber Reinforced Cement Composites 2 (HPFRCC 2), Proceedings of the Second International RILEM Workshop, Ann Arbor, USA, June, Edited by A.E. Naaman and H.W. Reinhardt, RILEM Publications s.a.r.l., Cachan Cedex, France, pp. 1-24.
12. Maalej, M., and Li, V.C. (1995), "Introduction of Strain Hardening Engineered Cementitious Composites in the Design of Reinforced Concrete Flexural Members for Improved Durability," ACI Structural Journal, Vol. 92, No. 2, March-April, pp. 167-176.
13. Li, V.C. (1993), "From Micromechanics to Structural Engineering – The Design of Cementitious Composites for Civil Engineering Applications," JSCE Journal of Structural Mechanics and Earthquake Engineering, Vol. 10, No. 2, pp. 37-48.
14. Naaman, A.E. (1999), "Fibers with Slip Hardening Bond," High Performance Fiber Reinforced Cement Composites 3 (HPFRCC 3), Proceedings of the Third International RILEM Workshop, Mainz, Germany, May, Edited by H.W. Reinhardt and A.E. Naaman, RILEM Publications s.a.r.l., Cachan Cedex, France, pp. 371-385.
15. Kim, K., and Parra-Montesinos, G. (2003), "Behavior of HPFRCC Low-Rise Walls Subjected to Displacement Reversals," High Performance Fiber Reinforced Cement Composites 4 (HPFRCC 4), Proceedings of the Fourth International RILEM Workshop, Ann Arbor, USA, June, Edited by A.E. Naaman and H.W. Reinhardt, RILEM Publications, s.a.r.l., Cachan Cedex, France, pp. 505-515.
16. Parra-Montesinos, G.J., and Wight, J.K. (2000), "Seismic Response of Exterior RC Column-to-Steel Beam Connections," Journal of Structural Engineering, ASCE, Vol.126, No. 10, pp. 1113-1121.
17. Soubra, K.S., Wight, J.K., and Naaman, A.E. (1993), "Cyclic Response of Fibrous Cast-in-Place Connections in Precast Beam-Column Subassemblages," ACI Structural Journal Vol. 90, No. 3, pp. 316-323.
18. Vasconez, R.M., Naaman, A.E., and Wight, J.K. (1998), "Behavior of HPFRCC Connections for Precast Concrete Frames under Reversed Cyclic Loading," PCI Journal, Vol. 43, No. 6, pp. 58-71.
19. Billington, S.L., and Yoon, J. (2002), "Cyclic Behavior of Precast Post-Tensioned Segmental Concrete Columns with ECC," Proceedings of the JCI International Workshop on Ductile Fiber Reinforced Cementitious Composites (DFRCC) – Applications and Evaluation (DFRCC-2002), Takayama, Japan, October, Japan Concrete Institute, Tokyo, Japan, pp. 279-288.
20. ACI Committee 318 (1999), "Building Code Requirements for Structural Concrete (318-99)," American Concrete Institute, Farmington Hills, Michigan.